

Supplementary information

Activating Electrode-Electrolyte Interface via a ZnO@Black Phosphorus Modulation Layer for Dendrite-Free Li Metal Anodes

Pengwei Li^a, Guodong Zhang^{a,b}, LiangPing Xiao^a, Kai Chen^a, Xingyun Li^{a,*}, Bin Han^a, Jiebin Qiu^a, Qingchi Xu^{a,*}, Jun Xu^{a,*}

^a Department of Physics, Research Institute for Biomimetics and Soft Matter, Fujian Provincial Key Laboratory for Soft Functional Materials, Xiamen University, Xiamen 361005, P. R. China

^b Department of Biomaterials, College of Materials, Xiamen University, Xiamen 361005, Fujian, China

Experimental Section

Exfoliation of Black Phosphorus (BP). Bulk black Phosphorus was exfoliated by an electrochemical approach. Briefly, bulk black phosphorus (500 mg) and a platinum sheet are fixed on the cathode and anode, respectively, in a two-electrode cell which contains 40 mL anhydrous organic electrolyte. The electrolyte was prepared by dissolving 1.6 g tetrabutylammonium hexafluorophosphate in 40 ml DMF. A stable working bias (-10 V) was applied between cathode and anode to trigger the exfoliation. Afterwards, the exfoliated flakes were centrifuged with DMF for 5 times, then dispersed into anhydrous DMF by mild sonication in the ice bath (2h). The as-prepared dispersion was centrifuged at 1500 rpm, 10 min to discard the suspended thick flakes and un-exfoliated large pieces. The brown supernatant was collected for further experiments.

Synthesis of Amorphous Zn Oxide on Black Phosphorus Nanosheets (ZnO@BP).

Zn(CH₃COO)₂·2H₂O (21.9 mg) and 15.5 mg BP were dispersed into 10 mL diethylene glycol. Then, the homogeneous mixture was transferred into a 20 mL Teflon lined autoclave. The autoclave was tightly sealed and transferred into a heating oven, kept at

150 °C for 0.5 h. When the reaction completed, the sample was collected by suction filtration, and washed at least three times by ethanol.

Fabrication of the BP and ZnO@BP modulation layer on Li metal anode.

To fabricate the ZnO@BP modulation layer on Li metal anode, 5 mg ZnO@BP was dispersed in 1 mL dimethyl carbonate to form a homogenous suspension, followed by drop-casting 100 μ L suspension onto Li metal (Diameter: 1.58 cm) in the argon-filled glove box. The ZnO@BP coated Li metal (ZnO@BP/Li) were dried at 80 °C for 24 h and cooled to room temperature for later use. For comparison, BP coated the Li metal (BP/Li) was also prepared through the similar processes.

Fabrication of the BP and ZnO@BP modulation layer on Cu foil.

5 mg ZnO@BP was dispersed in 1 mL solution composed of 950 μ L dimethyl carbonate and 50 μ L 5wt% nafion solution to form a homogenous suspension, followed by drop-casting 100 μ L suspension onto Cu foil (Diameter: 1.2 cm). The ZnO@BP coated Cu foils (ZnO@BP/Cu) were dried at 80 °C for 24 h and cooled to room temperature for later use. For comparison, BP coated Cu foils (BP/Cu) was also prepared through the similar processes.

Material Characterization. The morphologies of all the samples were characterized by scanning electron microscope ((SEM, Zeiss Gemini 500) and transmission electron microscope (TEM, Talos F200s). The thickness of 2D flakes was checked by Bruker Multimode 8 atomic force microscope (AFM). X-ray diffraction (XRD) patterns were recorded by an X-ray diffractometer (Bruker D8 Advance, 60 kV) using Cu $K\alpha$ ($\lambda=1.5406$ Å) as radiation. The Raman spectrum was measured using a LabRam HR

Evolution (HORIBA, Japan) Raman system, and the wavelength of the laser excitation is 532 nm. X-ray photoelectron spectroscopy (XPS) analysis was performed on a spectrometer (Escalab 250Xi, Thermo Fisher Scientific) using Al K α as the excitation source.

Electrochemical Measurements. All the electrochemical performances were evaluated by assembling 2032-type coin cells in the argon-filled glove box with O₂ and H₂O content below 0.1 ppm. The LiFePO₄ (LFP) cathodes was made by blending LFP, carbon black and polyvinylidene fluoride binder (PVDF) with a weight ratio of 8: 1: 1 (9: 0.5: 0.5 for high load) to form a slurry. The slurry was then blade-coated on the aluminum foils and dried in a vacuum oven at 60 °C for 12 h. The load of LFP was 3.2 mg cm⁻² and 10.8 mg cm⁻² for low load and high load, respectively. Li|Cu asymmetric cells with bare Cu foil, BP/Cu foil and ZnO@BP/Cu foil electrode were assembled with Li foil counter electrode. Li|Li symmetrical cells of bare Li, BP/Li and ZnO@BP/Li anode were assembled using two identical electrodes. 50 μ L of 1.0 M lithium bis(trifluoromethanesulfonyl)imide (LiTFSI) in 1,3-dioxolane/1,2-dimethoxyethane (DOL/DME, v:v=1:1) solution with 2 wt% LiNO₃ additive was used in Li|Cu asymmetric cells and Li|Li symmetrical cells. For full cells, the bare Li, BP/Li and ZnO@BP/Li were used as the anodes and Celgard 2400 was used as the separator. 60 μ L of 1.0 M LiPF₆ in ethylene carbonate/diethyl carbonate solution (EC/DEC, v:v=1:1) with 10% fluoroethylene carbonate (FEC) and 1% vinylene carbonate (VC) was added in the full cell. The average mass of each Li foil is 45.6 mg, so the N/P values under low and high LFP loads of the full cells are calculated to be 286.34 and 90.90,

respectively. And the E/C values of the full cells under low and high LFP loads are 97.61 and 30.99 $\mu\text{L mAh}^{-1}$, respectively. The electrochemical impedance spectroscopy (EIS) measurements and Tafel curve were conducted by using a Chenhua CHI 660E electrochemical workstation. Galvanostatic charge/discharge tests were performed on a LAND CT2001C battery tester system.

Li deposition activation energy. The activation energy for Li deposition was measured via temperature-dependent electrochemical impedance spectroscopy (EIS) tests on Li|Li symmetric cell. The EIS characterization was taken under different temperatures from 283.15 to 313.15 K. Data obtained from all cases were fitted to straight lines using the Arrhenius equation:

$$\frac{T}{R_{SEI}} = A \exp\left(-\frac{E_a}{RT}\right)$$

where E_a is the activation energy, T is the absolute temperature, R is the gas constant, R_{SEI} is the SEI film resistance, and A is the pre-exponential factor.

Li⁺ conductivity. The ionic conductivity was measured in Li|Cu asymmetric cells by electrochemical impedance spectroscopy (EIS) tests. The ionic conductivity is calculated by the following equation:

$$\sigma = \frac{l}{R_b \cdot S}$$

where σ represents the ionic conductivity, l represents to the thickness of BP or ZnO@BP coating film, R_b refers to the bulk resistance, and S is the area of the blocking electrode.

Li⁺ transference number. Li⁺ transference number (t_+) is evaluated by the potentiostatic polarization (PP) method. A small constant potential (10 mV) is applied on the Li

symmetric cell, and the current is recorded from the initial state (I_0) to the steady state (I_s) during the polarization process. Simultaneously, the charge transfer resistance (R_{ct}) before and after polarization were measured and denoted as R_0 and R_s , respectively.

The t_+ value was calculated by following equation:

$$t_+ = \frac{I_s(\Delta V - I_0 R_0)}{I_0(\Delta V - I_s R_s)}$$

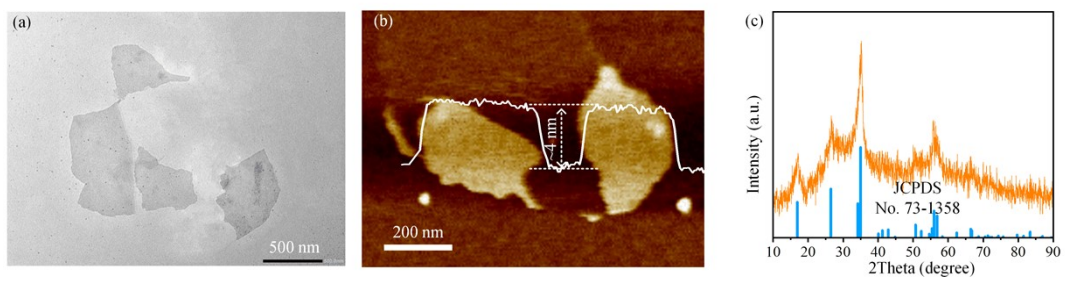


Fig. S1 (a) TEM and (b) AFM images of BP, (c) XRD pattern of BP.

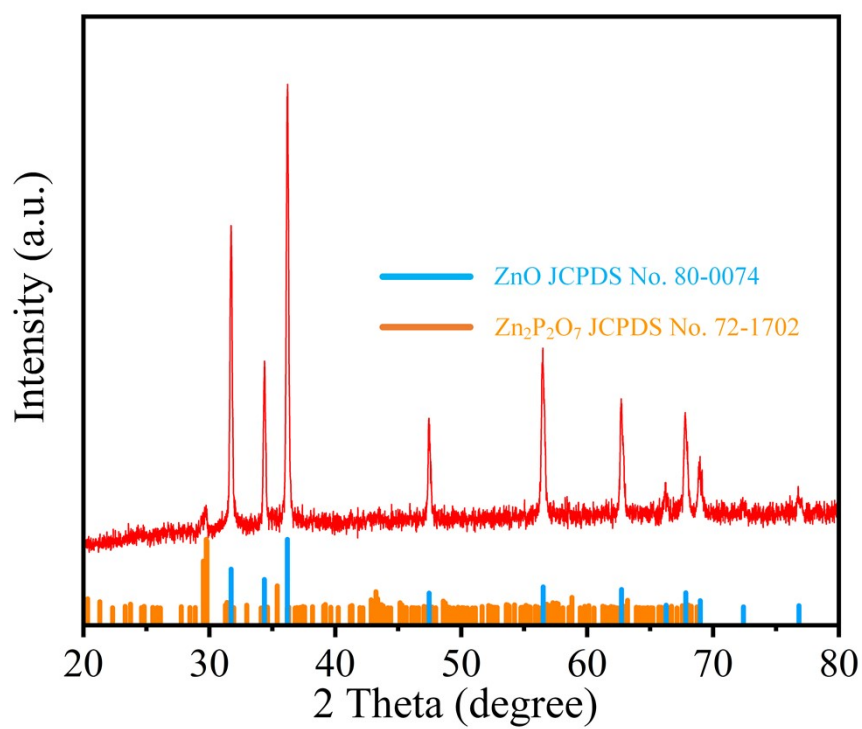


Fig. S2 XRD pattern of annealed ZnO@BP at 800 °C in Ar.

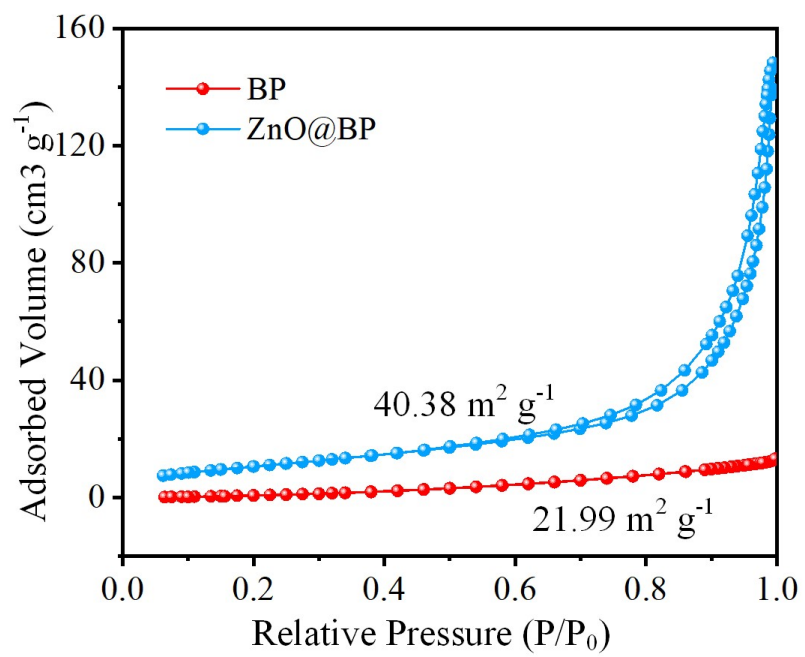


Fig. S3 N₂ adsorption/desorption curves of BP and ZnO@BP.

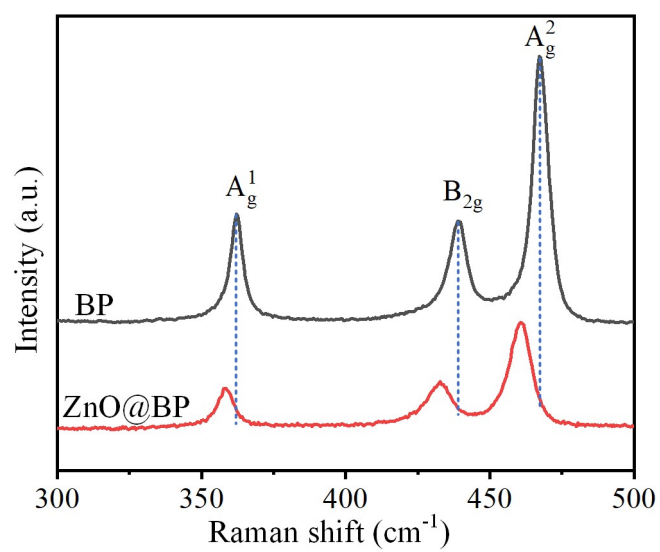


Fig. S4 Raman spectrum of bare BP and Zn@BP nanosheets.

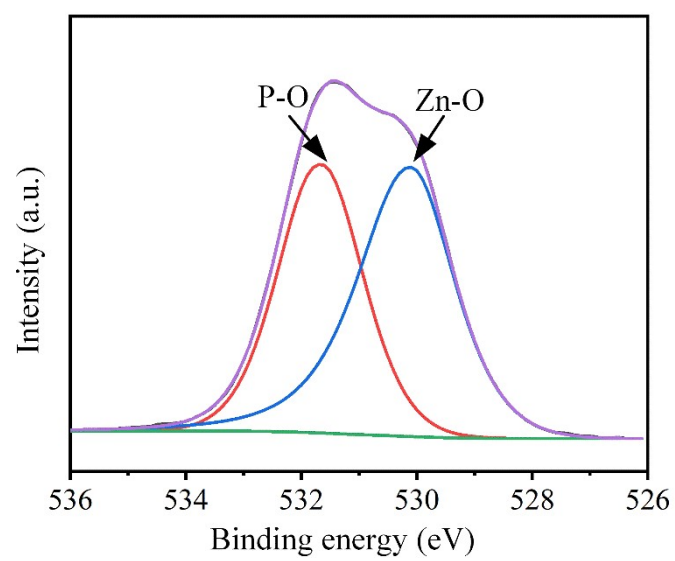


Fig. S5. O 1s XPS spectra of ZnO@BP.

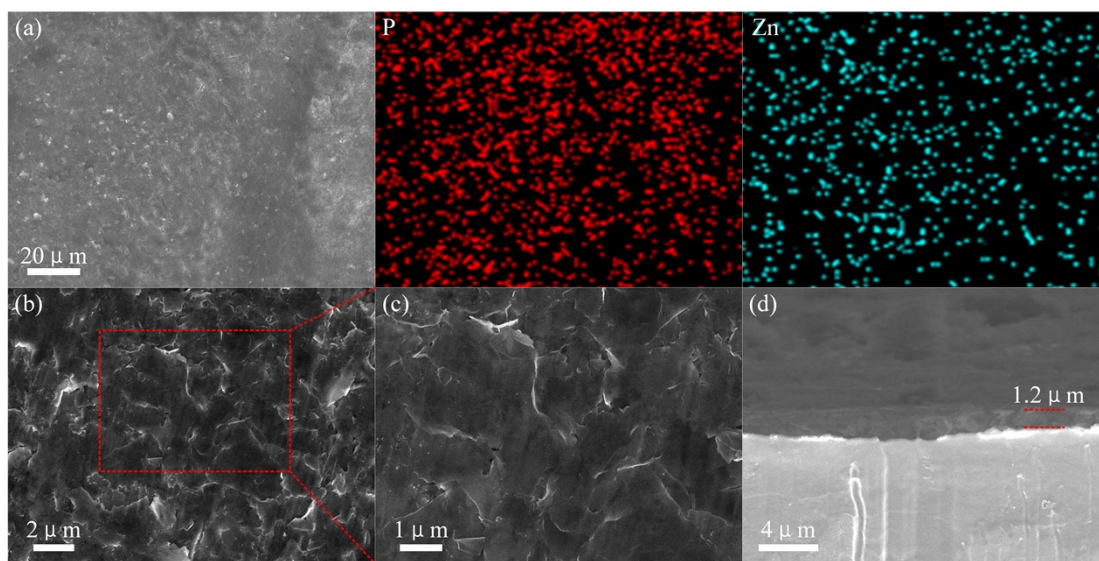


Fig. S6. (a) SEM EDS mapping, (b, c) Further amplified SEM and (d) cross-section image of the ZnO@BP/Li electrode.

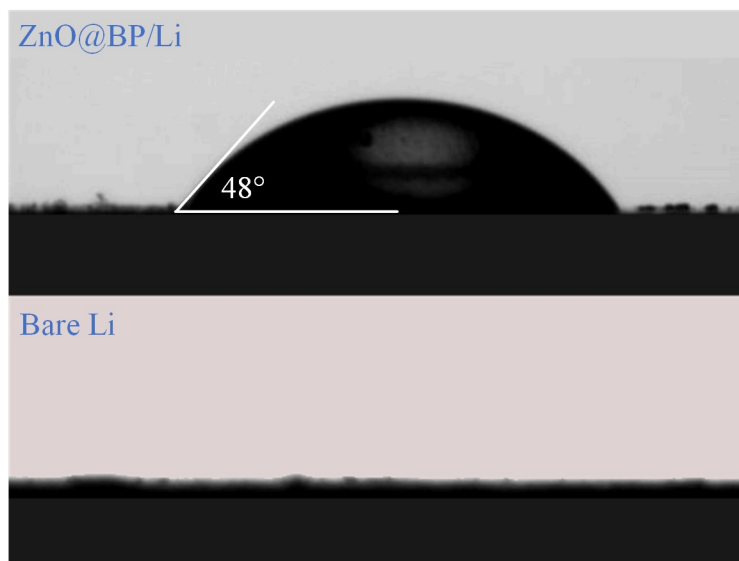


Fig. S7. Contact angle between the electrolyte and ZnO@BP/Li and bare Li

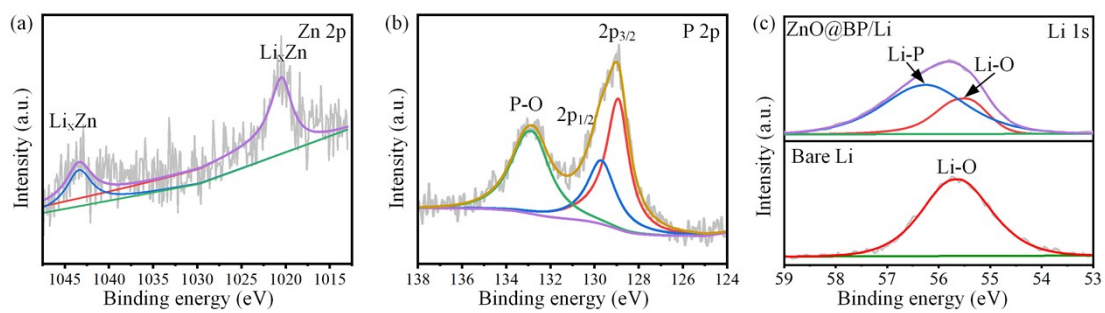


Fig. S8 (a) Zn 2p, (b) P 2p and (c) Li 1s XPS spectra of bare Li and ZnO@BP/Li.

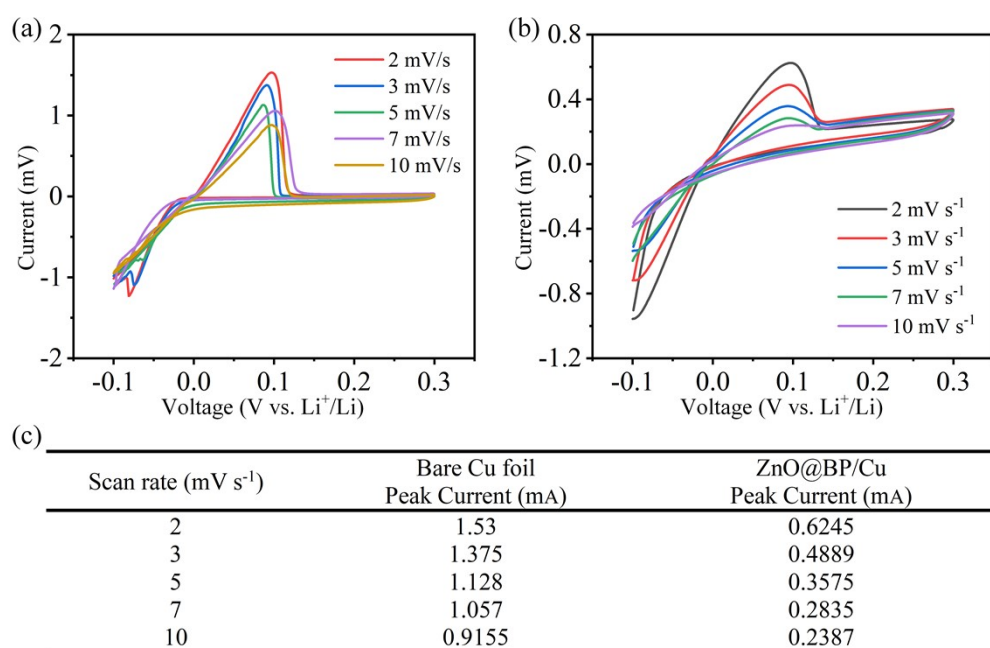


Fig. S9 (a, b) Cyclic voltammetry and (b) corresponding oxidative peak currents of Li-Cu cells with bare Li, BP/Li and ZnO@BP/Li anode.

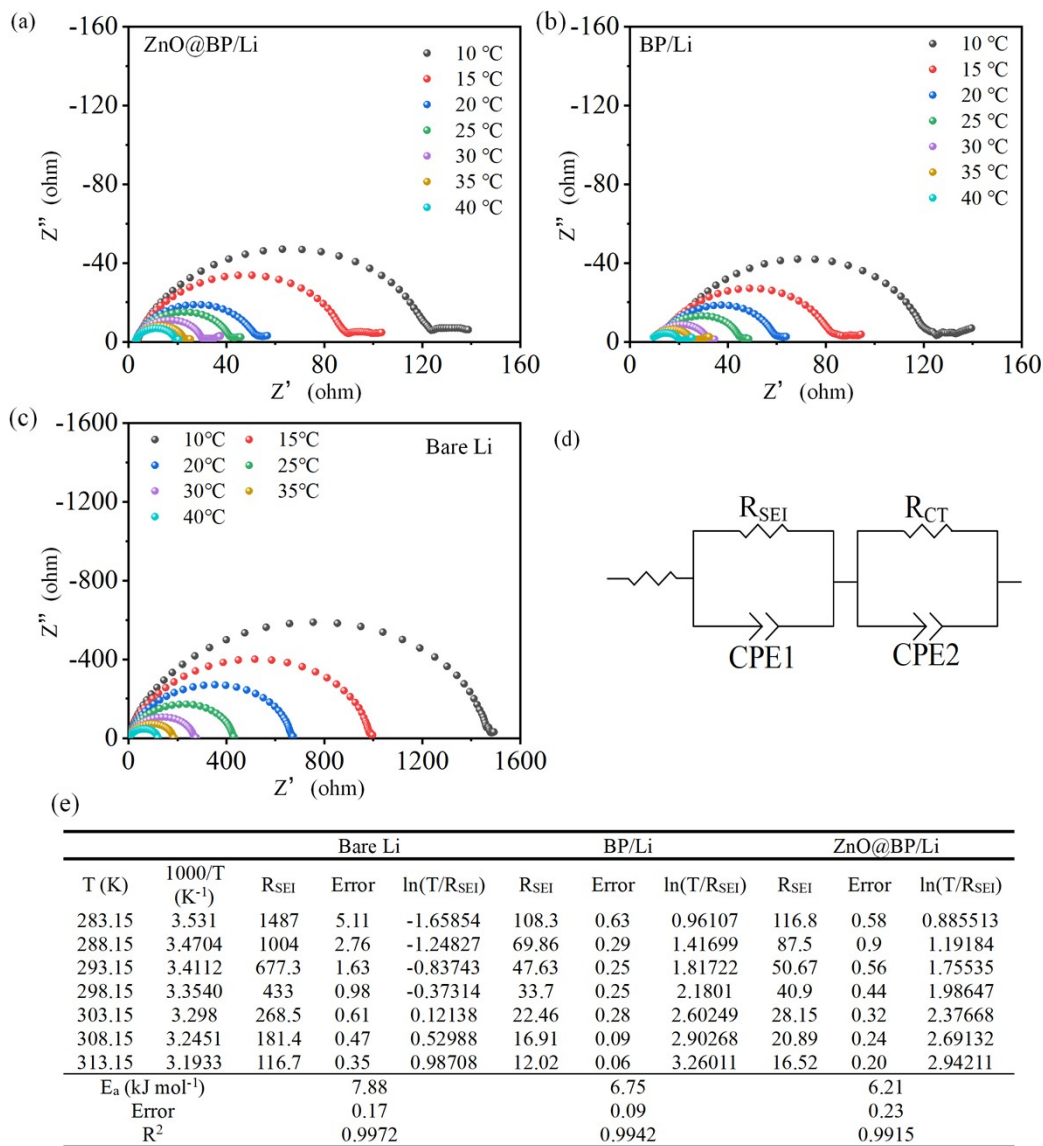


Fig. S10 Nyquist Plots at various temperatures for symmetric cells with (a) ZnO@BP/Li, (b) BP/Li and (c) bare Li, (d) the equivalent circuit model used for fitting. (e) Corresponding values of R_{SEI} under various temperatures.

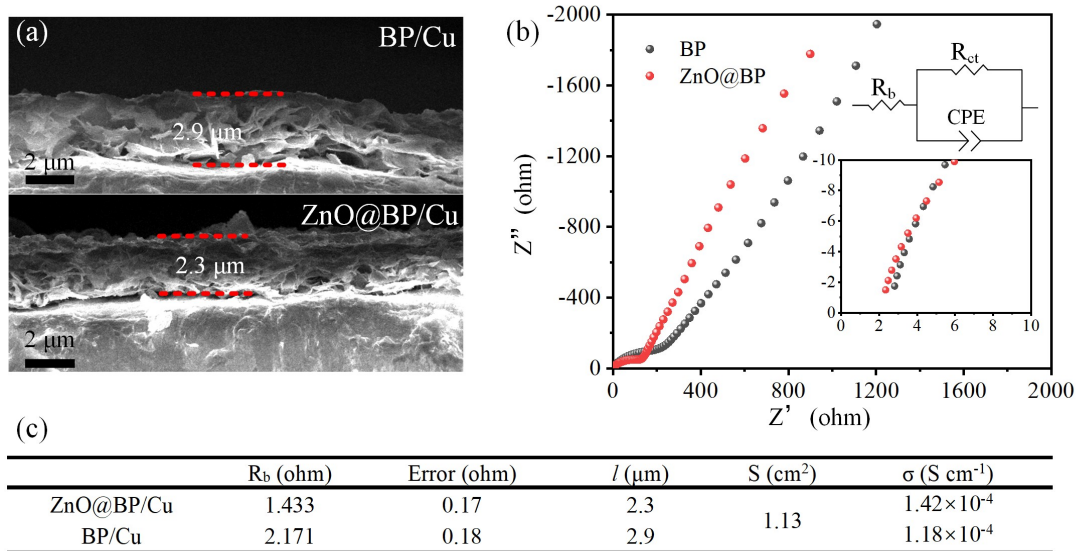


Fig. S11 (a) Cross-section SEM images of BP/Cu and ZnO@BP/Cu, (b) The EIS spectra of the BP/Cu|Li and ZnO@BP/Cu|Li cells, the inset of (b) is the equivalent circuit model used for fitting, (c) Corresponding values of R_b and calculated Li^+ conductivities.

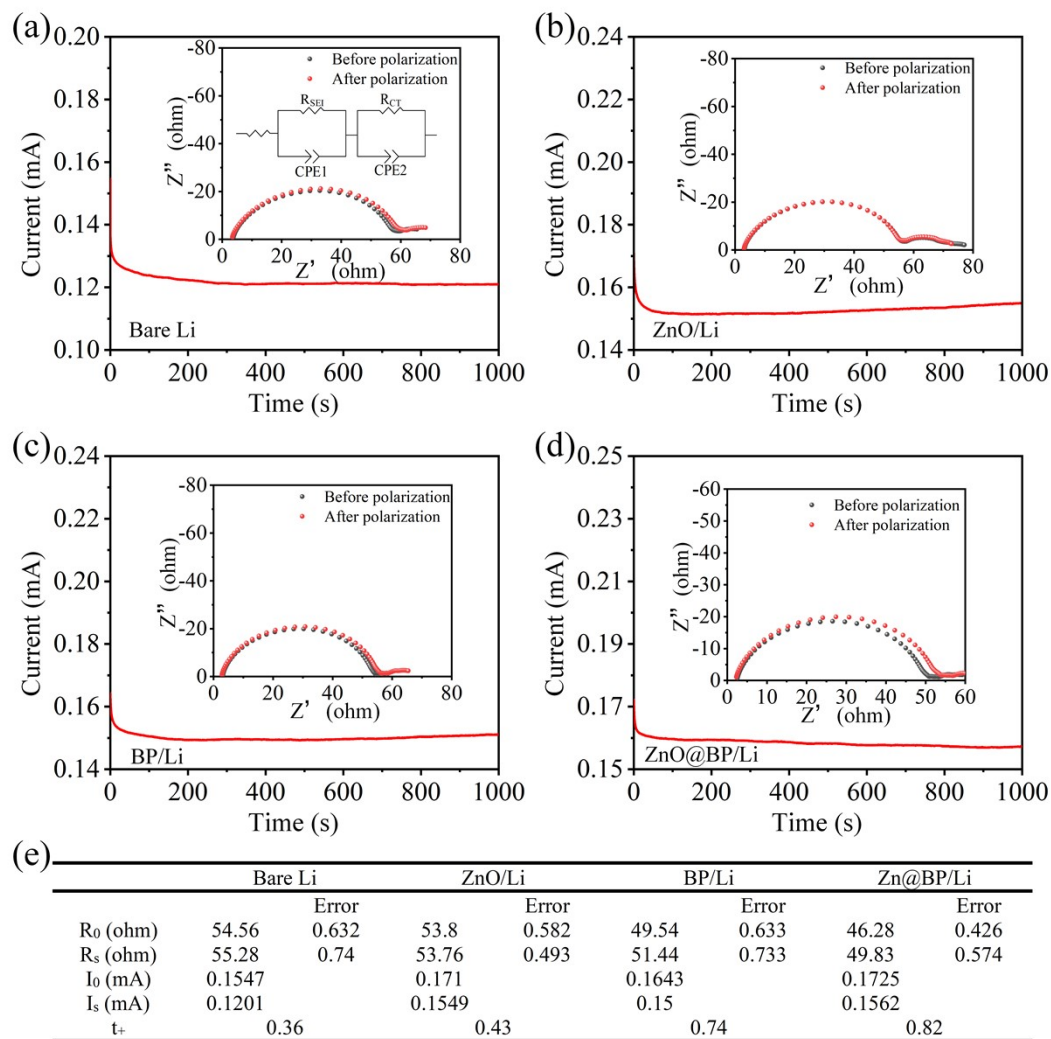


Fig. S12 Current-time plots of the fresh symmetric cells with bare (a) Li, (b) ZnO/Li, (c) BP/Li and (d) ZnO@BP/Li after the application of a constant potential (10 mV). The inserts are the EIS spectra before and after polarization and equivalent circuit model for fitting. (e) Corresponding values of initial current, steady-state current, initial resistance, steady-state resistance, and Li^+ transference number (t_+).

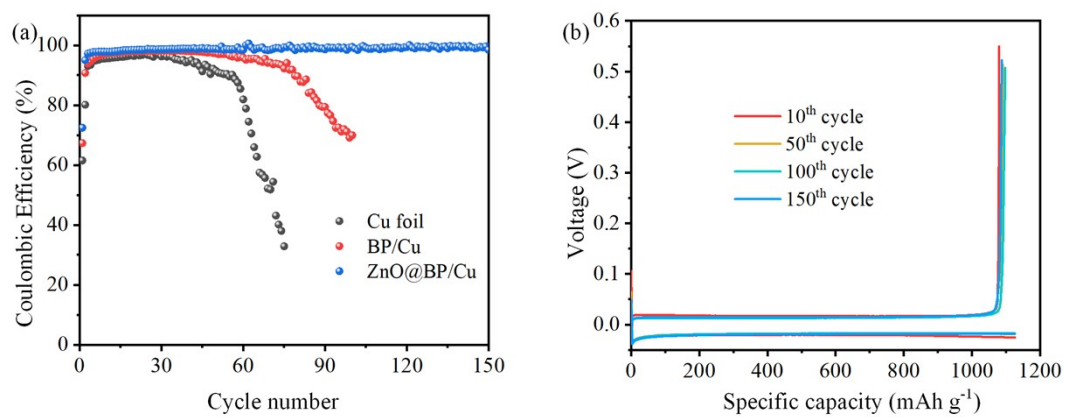


Fig. S13 (a) Coulombic efficiency of the Li|Cu cells with bare Cu, BP/Cu and ZnO@BP/Cu electrodes at the current density of 1 mA cm⁻² with a capacity of 1 mAh cm⁻². (b) Voltage curves of the Li|Cu cells with the ZnO@BP/Cu electrode at different cycles.

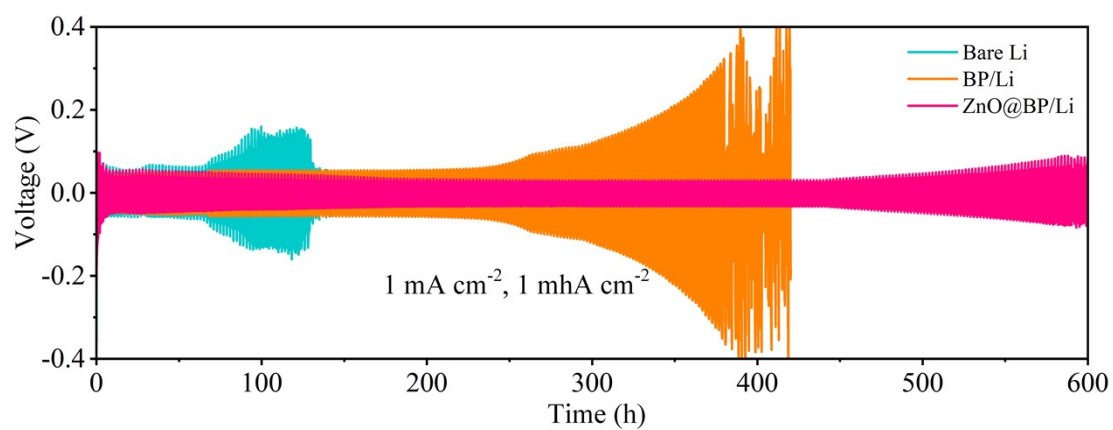


Fig. S14 Cyclic performance of symmetric cells with bare Li, BP/Li and ZnO@BP/Li in EC/DEC electrolyte at 1 mA cm^{-2} for 1 mAh cm^{-2} .

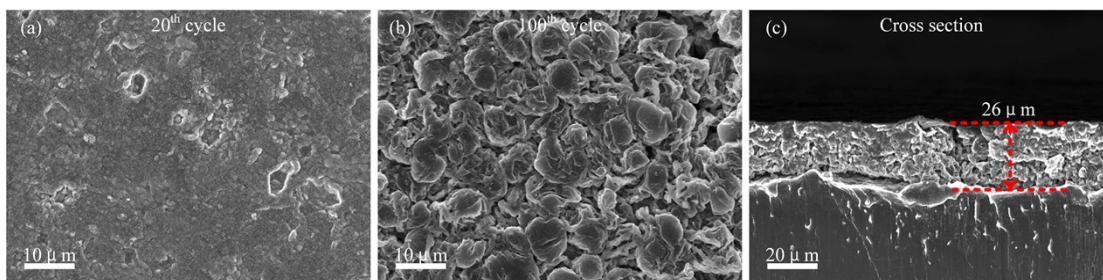


Fig. S15 EX-situ SEM images of BP/Li disassembled from symmetric cell after cycle. Top view of BP/Li electrode after (a) 20 cycles, (b) 100 cycles. Cross sections of (c) BP/Li and electrode after 100 cycles.

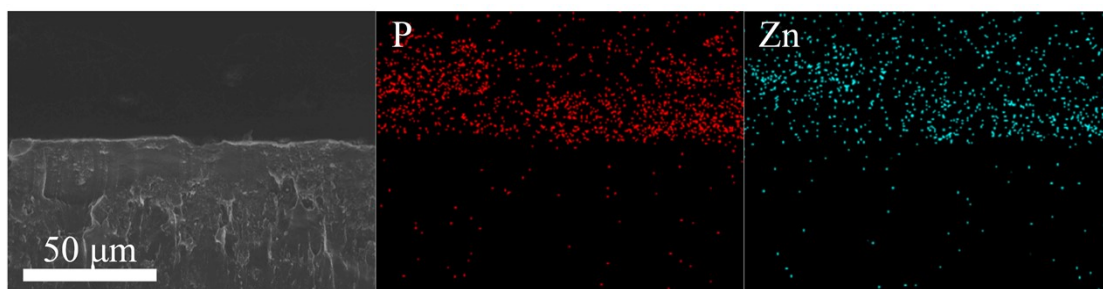
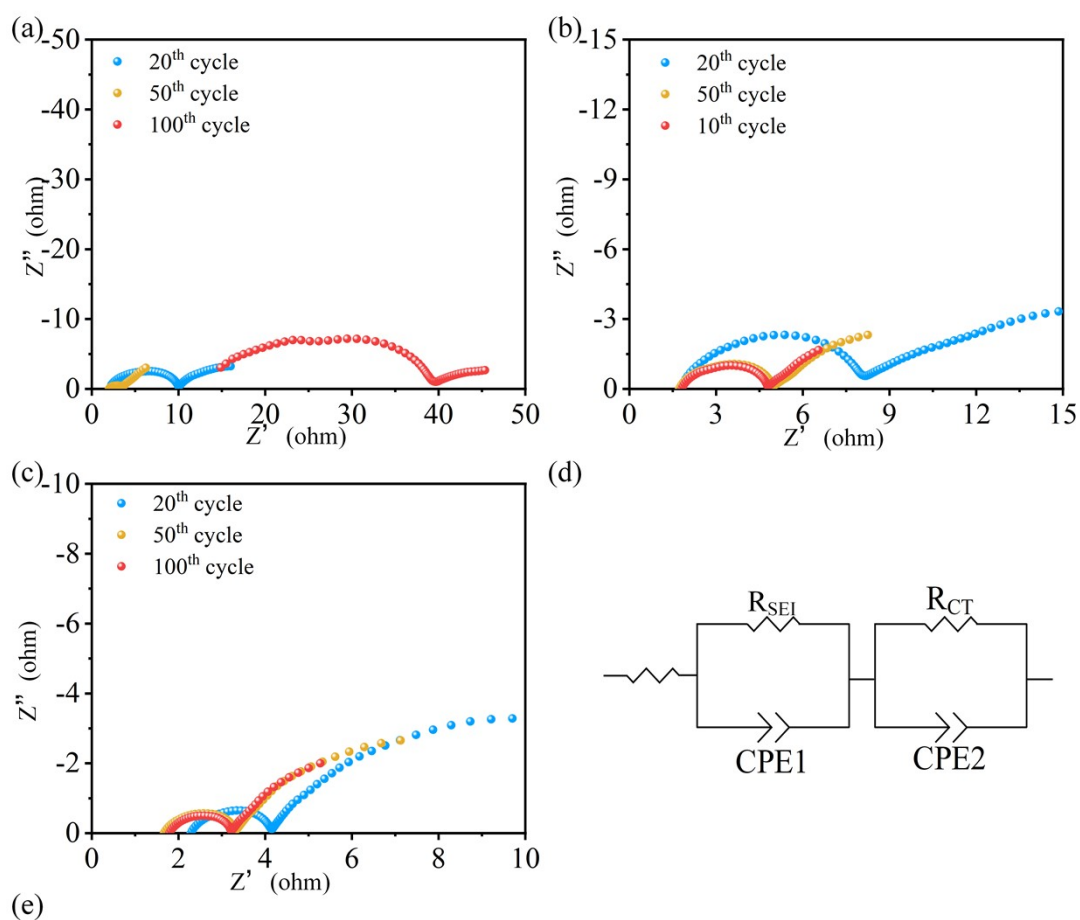


Fig. S16 Cross-section SEM EDS mapping of ZnO@BP/Li after 100 cycles.



	Li (ohm)				BP/Li (ohm)				ZnO@BP/Li (ohm)			
	R_{SEI}	Error	R_{ct}	Error	R_{SEI}	Error	R_{ct}	Error	R_{SEI}	Error	R_{ct}	Error
20 th cycle	6.53	0.27	7.54	0.092	4.80	0.31	6.14	0.031	1.10	0.081	1.605	0.009
50 th cycle	0.97	0.051	1.36	0.015	2.08	0.186	2.83	0.028	1.14	0.109	1.39	0.015
100 th cycle	25.12	0.787	20.22	0.141	2.02	0.183	2.65	0.024	1.13	0.104	1.30	0.012

Fig.S17 (a-c) EIS spectra of the symmetric cells with different electrodes after 20, 50 and 100 cycles at 1 mA cm^{-2} for 1 mAh cm^{-2} , (d) The equivalent circuit model used for fitting, (e) Corresponding values of R_{SEI} and R_{ct} .

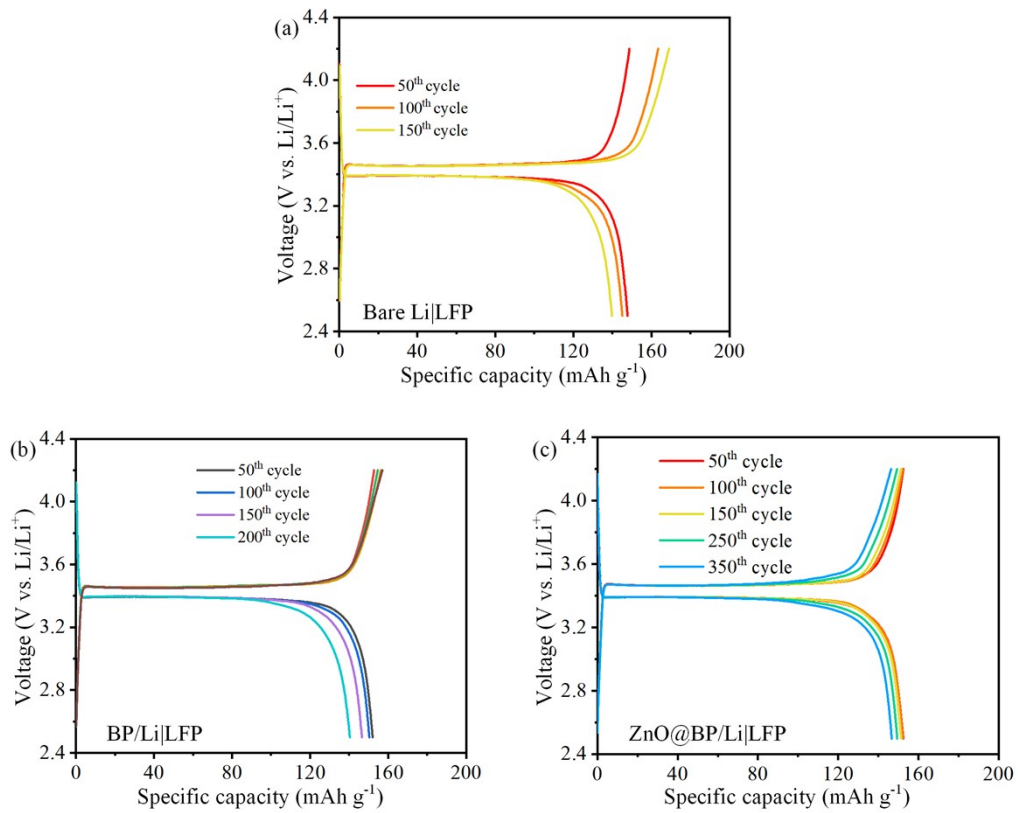


Fig. S18 Voltage profiles of bare Li|LFP, BP/Li|LFP and ZnO@BP/Li|LFP full cells at 0.5C.

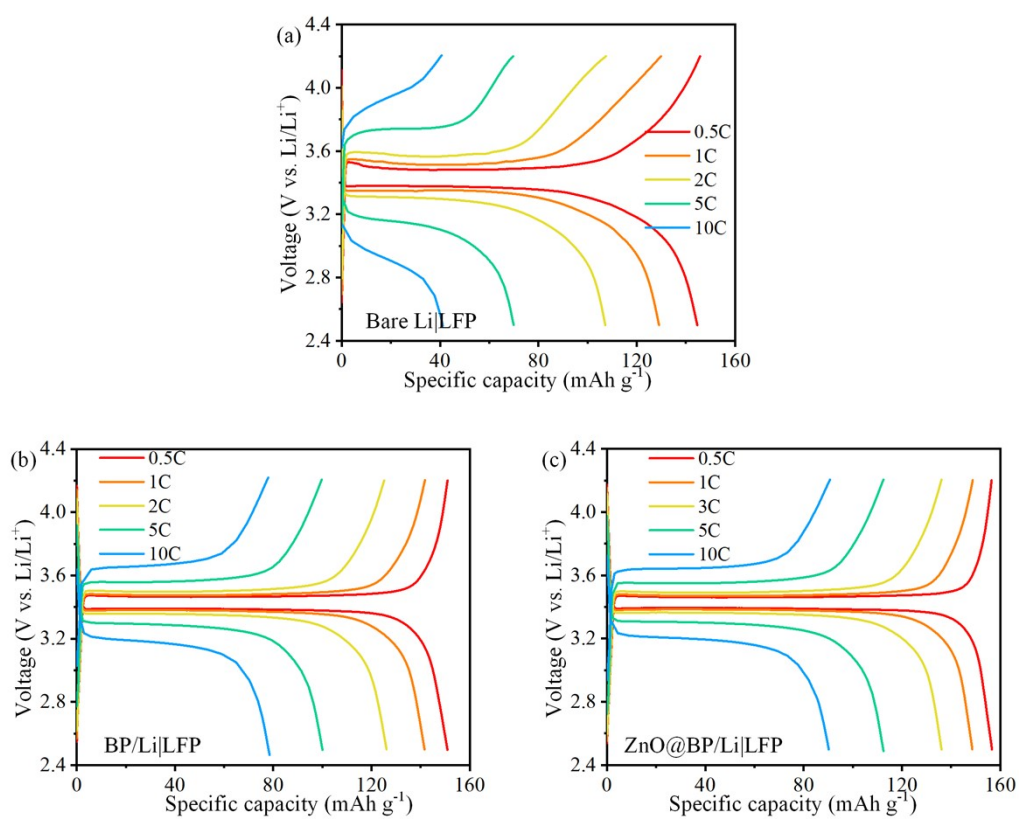


Fig. S19 Voltage profiles of bare Li|LFP, BP/Li|LFP and ZnO@BP/Li|LFP full cells at various rates from 0.5 to 10 C.

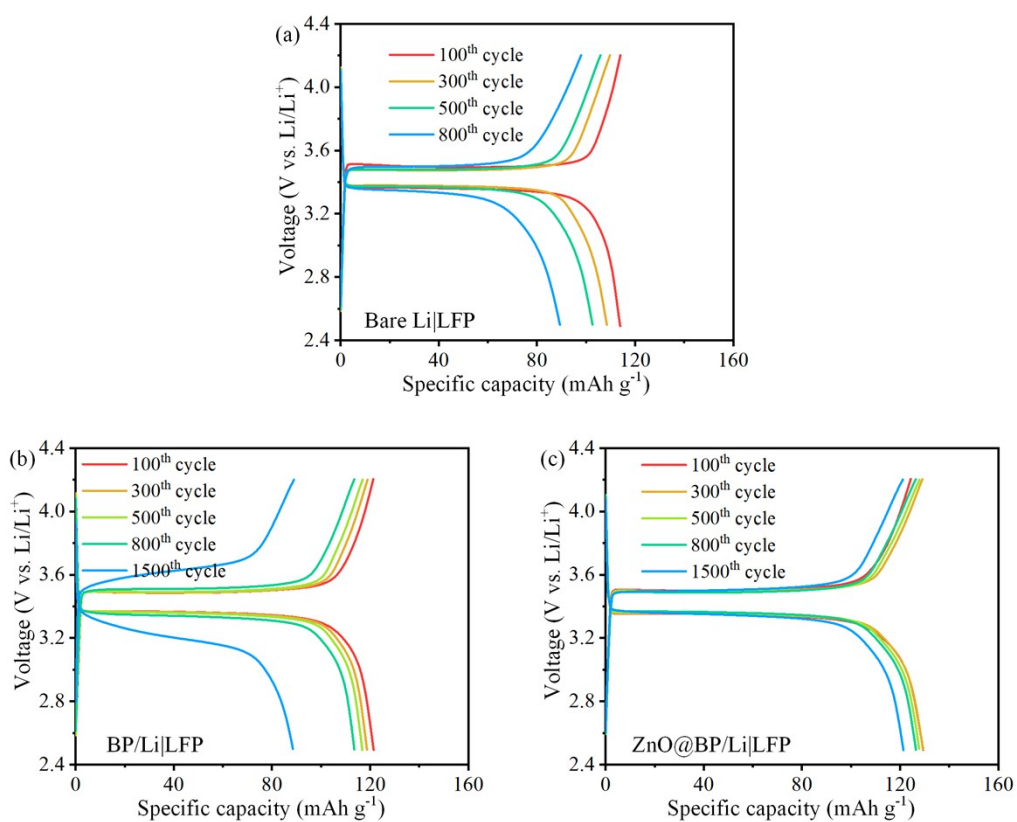


Fig. S20 Voltage profiles of bare Li|LFP, BP/Li|LFP and ZnO@BP/Li|LFP full cells at 2C.

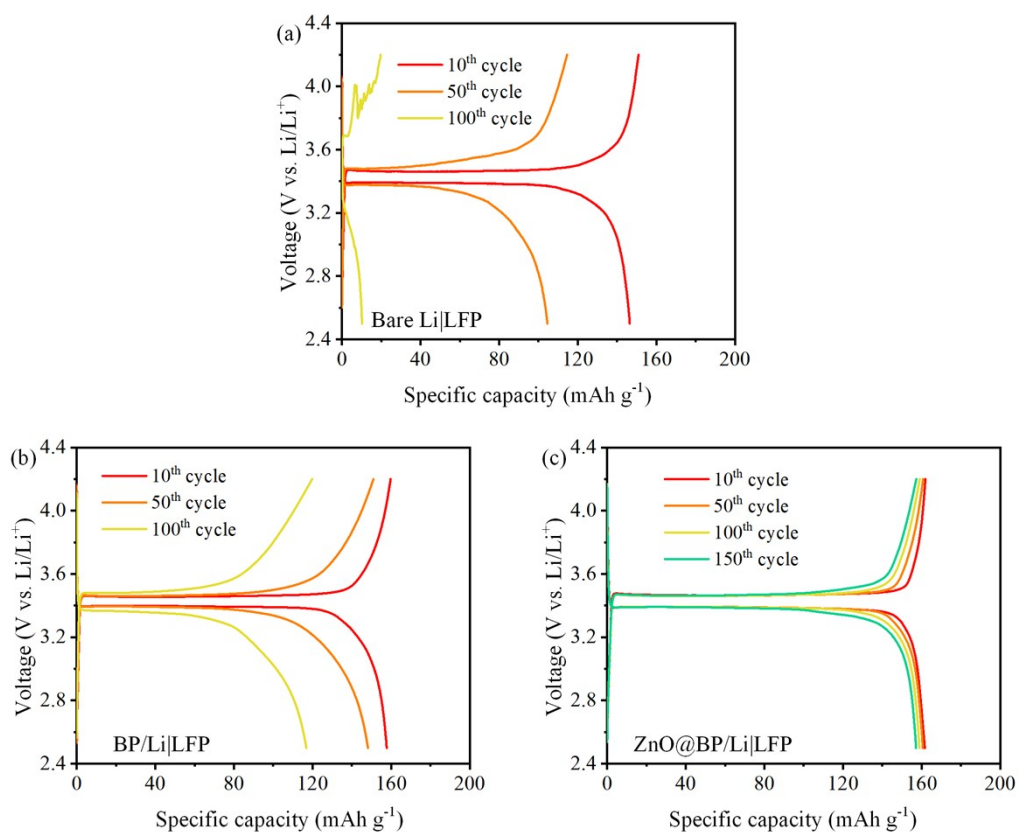


Fig. S21 Voltage profiles of bare Li|LFP, BP/Li|LFP and ZnO@BP/Li|LFP full cells at 0.2C.

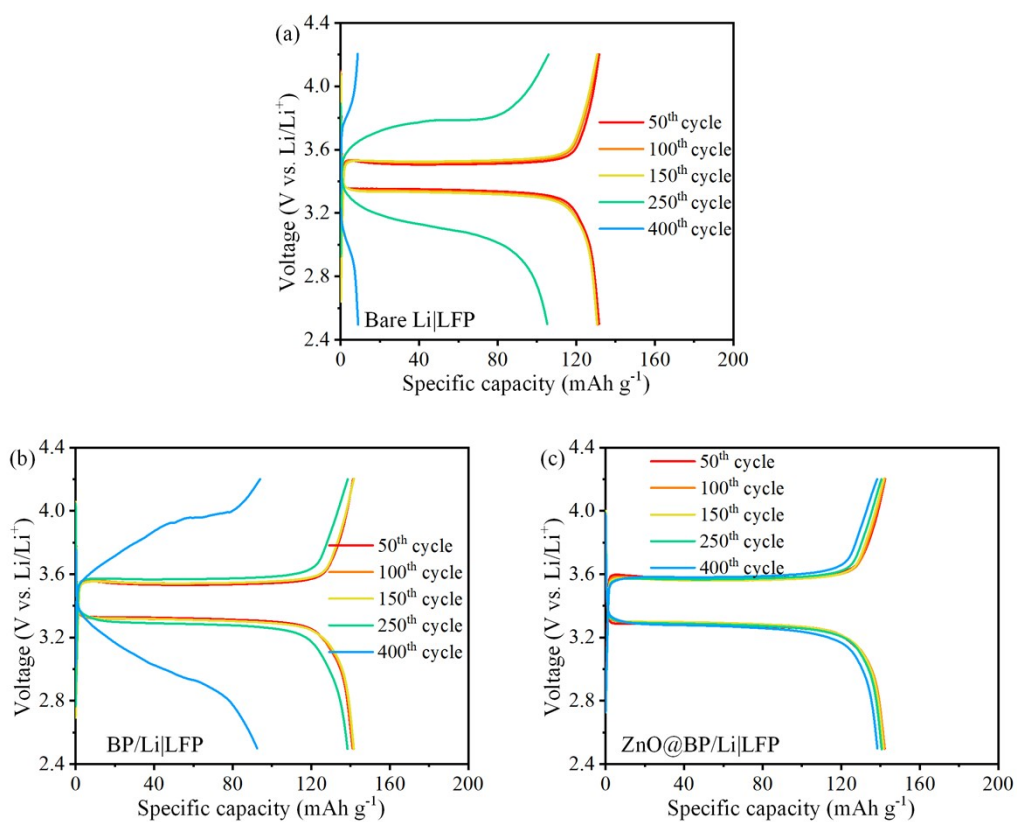


Fig. S22 Voltage profiles of bare Li|LFP, BP/Li|LFP and ZnO@BP/Li|LFP full cells at 1C.

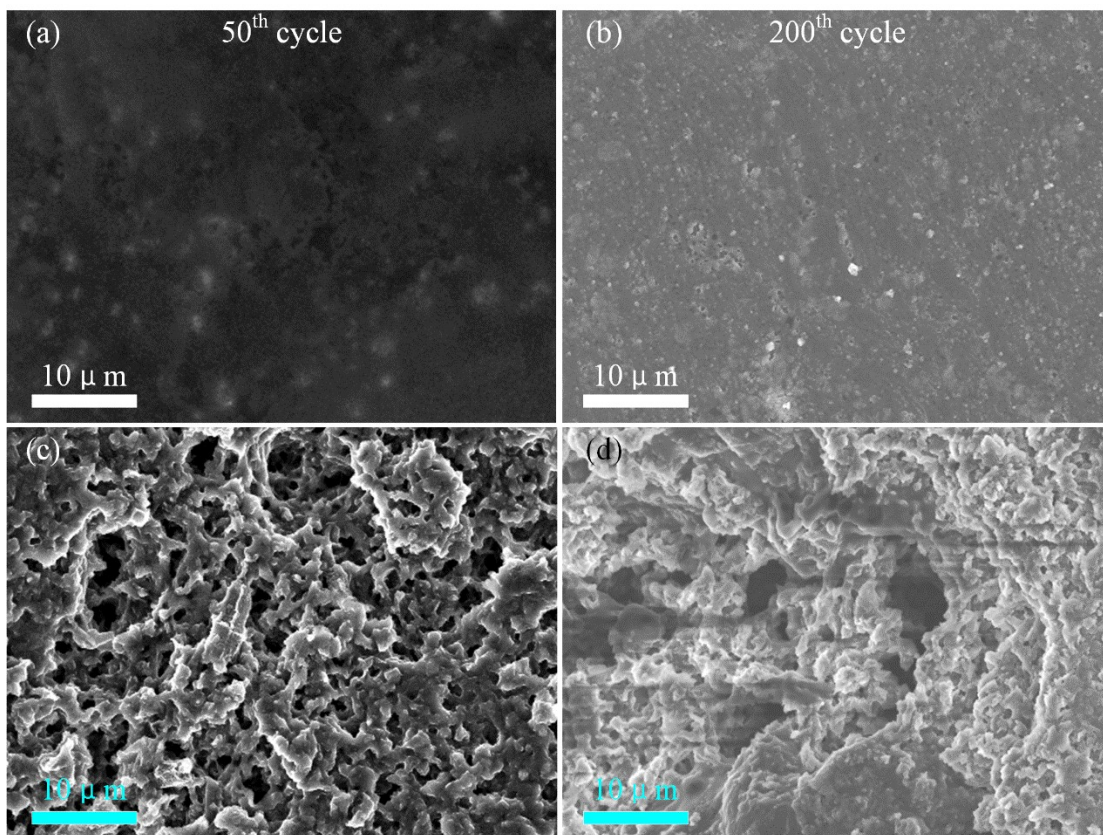


Fig. S23 EX-situ SEM images of bare Li and ZnO@BP/Li disassembled from Li|LFP full cells after cycle. (a, b) Top view of ZnO@BP/Li anode after (a) 50 cycles, (b) 200 cycles. (c-d) Top view of bare Li anode after (c) 50 cycles, (d) 200 cycles.